The Green's Function Density Functional Tight-Binding (gDFTB) Method for Molecular Electronic Conduction[†]

Jeffrey R. Reimers,*,[⊥] Gemma C. Solomon,[⊥,@] Alessio Gagliardi,[‡,§] Ante Bilić,[⊥,#]
Noel S. Hush,[⊥,£] Thomas Frauenheim,[§] Aldo Di Carlo,[¶] and Alessandro Pecchia[¶]

School of Chemistry, The University of Sydney, NSW 2006, Australia, PaSCO Graduate School, University of Paderborn, D-33098 Paderborn, Germany, Bremen Center for Computational Materials Science, University of Bremen, D-28359 Germany, School of Molecular and Microbial Biosciences, The University of Sydney, NSW 2006, Australia, and Department of Electronic Engineering, University of Rome "Tor Vergata", Italy

Received: January 23, 2007; In Final Form: April 8, 2007

A review is presented of the nonequilibrium Green's function (NEGF) method "gDFTB" for evaluating elastic and inelastic conduction through single molecules employing the density functional tight-binding (DFTB) electronic structure method. This focuses on the possible advantages that DFTB implementations of NEGF have over conventional methods based on density functional theory, including not only the ability to treat large irregular metal−molecule junctions with high nonequilibrium thermal distributions but perhaps also the ability to treat dispersive forces, bond breakage, and open-shell systems and to avoid large band lineup errors. New results are presented indicating that DFTB provides a useful depiction of simple gold−thiol interactions. Symmetry is implemented in DFTB, and the advantages it brings in terms of large savings of computational resources with significant increase in numerical stability are described. The power of DFTB is then harnessed to allow the use of gDFTB as a real-time tool to discover the nature of the forces that control inelastic charge transport through molecules and the role of molecular symmetry in determining both elastic and inelastic transport. Future directions for the development of the method are discussed.

Introduction

The theory, implementation, and application of our nonequilibrium Green's function (NEGF)-based method for use in molecular electronics calculations is described. While most NEGF approaches[1−5] make use of density functional theory (DFT) to evaluate elements of the molecular electronic structure,[6−10] our developments[3−5] and applications[11−14] introduce a new NEGF implementation called "gDFTB" based on the density functional tight-binding[15,16] (DFTB) model electronic Hamiltonian. The initially attractive feature of gDFTB comes from its combination of the most general formalism currently available for molecular electronics with an efficient computational scheme that can allow very large systems to be treated. To date, our aims have focused on demonstrating that the technique works rather than on its application to new areas such as heat flow, device operating temperature prediction, and so forth, features that will be critical in any practical engineering application of molecular electronics but, at the moment, are beyond experimental scientific investigation. Indeed, gDFTB is a technique designed for applications in nanotechnology, applications that are pertinent to systems having components that are both intrinsically molecular in nature, requiring treatment by quantum chemical techniques, and intrinsically macroscopic in nature, requiring treatment of integrated solid-state electronics.

Much of this paper presents a review of the development of gDFTB, including a brief introduction to the field of molecular electronics, limitations of standard DFT approaches, the DFTB electronic structure alternative, and the gDFTB method. While previously we have emphasized the mathematical formalism, the requirements of an accurate electronic structure method, and applications interpreting experimental data, this review concentrates on the role of DFTB, its promises, problems, and achievements. In particular, the enhanced computational efficiency of DFTB compared to that of DFT is shown to lead to potential or demonstrated applications in finding realistic geometries and structures for irregular high-temperature devices and for ascertaining physical principles from inside the complex NEGF theory that describes single-molecule conductivity in simple terms. How gDFTB has been used to identify the role played by molecular symmetry will be described. New results are also presented concerning the accuracy of DFTB in predicting chemisorbed structures on gold, as well as results providing symmetry assignments of observed inelastic scattering data. The means by which symmetry has been implemented in DFTB is also described for the first time, along with the advantages obtained for general applications of symmetry-enabled DFTB. These include significant enhancements in computational efficiency with associated reduction of numerical instability.

The DFTB Electronic Structure Method

The density functional tight-binding method presents a second-order approximation to density functional theory[15] that

---

† Part of the "DFTB Special Section".

* To whom correspondence should be addressed. E-mail: reimers@chem.usyd.edu.au.

⊥ School of Chemistry, The University of Sydney.

‡ University of Paderborn.

§ University of Bremen.

£ School of Molecular and Microbial Biosciences, The University of Sydney.

¶ University of Rome "Tor Vergata".

@ Current address: Department of Chemistry, Northwestern University, Evanston, IL 60208-3113, U.S.A.

Current address: School of Applied Chemistry, Curtin University of Technology, P.O. Box U1987, Perth WA 6845, Australia.

DFTB for Molecular Electronics

J. Phys. Chem. A, Vol. 111, No. 26, 2007 **5693**

is highly computationally efficient and, hence, well suited to large systems. Recently, an enhanced version of this method involving self-consistent charge description, the self-consistent-charge density functional tight-binding method (SCC-DFTB), has emerged. This enhancement significantly improves the transferability and generality of this approach through the proper treatment of intramolecular charge flow and polarization,[16] effects that are, in general, very important in molecular electronics. All calculations reported herein involve this functionality. While many of the properties of the DFTB Hamiltonian are specified a priori through the perturbation theory expansion, some adjustable parameters remain and, for each pair of atoms in the system, must be determined explicitly. Well-tested parameters are commonly available for the atoms H, C, N, O, S, and Zn[17] only, and we have developed parameters for Au,[3,12] enabling applications involving gold atoms and electrodes. While DFTB was originally developed for materials applications, applications in biological areas are now much more extensively developed.[16,19−24]

The two main approximations in standard DFTB are the use of a minimal basis set of valence atomic orbitals in order to reduce the matrix dimensions and, furthermore, calculation of the integrals entering the matrices within the two-center approximation.[15] Therefore, the non-self-consistent part of the pair integrals is calculated at a step previous to the actual simulation and tabulated as a function of the interatomic distance for each different pair of atomic species. The starting electronic density is expanded as a sum of a reference density, $n_0(r)$ (that can be chosen as the superposition of neutral atomic densities), and a deviation, $\delta n(r)$, such that $n(r) = n_0(r) + \delta n(r)$. The total energy of the system can be described, up to second order in the local density fluctuations, as

$$E_{\text{tot}}(n) = \sum_k n_k < \phi_k|\mathbf{H}_0|\phi_k > + E_{\text{rep}}(n_0) + E^{(2)}(\delta n) \quad (1)$$

The first term is the sum of the single-particle eigenstates with respect to a zero-order Hamiltonian

$$\mathbf{H}_0 = \mathbf{T} + \mathbf{V}_{\text{eff}}(n) \quad (2)$$

where $\mathbf{T}$ is the kinetic operator and $\mathbf{V}_{\text{eff}}$ an effective potential which depends only on the zero-order density. Neglecting the three-center integrals, the expansion of these terms in the local basis can be calculated in advance for every atom pair and tabulated for fast look-up during the calculation.

The second term in eq 1, E_{rep}, is a repulsive term which takes into account the core−core repulsion and removes the double counting of terms that appear in both the first contribution to the total energy (derived from $\mathbf{H}_0$) and in the third contribution, $E^{(2)}(\delta n)$. In effect, E_{rep} can be thought of as a short-range repulsive contribution to the energy. It is evaluated as a sum of atomic pairs contributions[25]

$$E_{\text{rep}}(n) = \frac{1}{2} \sum_{\alpha\beta} U_{\alpha\beta}(n_\alpha, n_\beta) \quad (3)$$

where α and β index the valence atomic orbitals and $U_{\alpha\beta}$ are the calculated differences between DFT-calculated interaction energies and the electronic part of the energy of the DFTB energy, as evaluated for a chosen set of molecules. These contributions for each atom pair are evaluated over a range of interatomic spacings and saved in spline form in a look-up table for speedy evaluation.

Finally the third term, $E^{(2)}(\delta n)$, is a self-consistent term which includes the correction to the energy induced by the charge redistribution between atoms after bonding. To second order, this correction is formally

$$E^{(2)} = \frac{1}{2} \int \int \left(\frac{1}{|r - r'|} + \frac{\delta^2 E_{\text{xc}}}{\delta n \delta n'} \right) \delta n \delta n' \, \mathrm{d}r\mathrm{d}r' \quad (4)$$

where $\mathbf{r}$ and $\mathbf{r}'$ are the locations of pairs of electrons and E_{xc} is the exchange correlation potential, but this term is then greatly simplified by retaining only the monopole term in the radial expansion of the atom-centered density fluctuations[25]

$$\delta n \approx \Delta q_i \frac{F_{00}^i(\mathbf{r} - \mathbf{R}_i)}{4\pi} \quad (5)$$

where q_i are the atomic charges, $\mathbf{R}_i$ are the locations of the nuclei, and F_{00}^i is the normalized radial dependence of the density fluctuation on atom i. The normalized spherical charge density at each atomic center is assumed to have a simple exponential decay of the form[26]

$$E^{(2)} = \frac{1}{2} \sum_{ij} \Delta q_i \Delta q_j \gamma_{ij} \quad (6)$$

where γ_{ii} at $R = 0$ is the difference between the atomic ionization potentials and electron affinities (often identified as the parameter "U" in the Hubbard electronic structure model), while γ_{ij} reduces to the Coulomb repulsion $1/R_{ij}$ for atoms interacting at long distance.

Molecular Electronics

Molecular electronics is a field inspired by the original predictions of Aviram and Ratner[27] in which single molecules could carry and rectify current. Early developments of the field have been reviewed,[28] as have recent developments,[5] many of which were inspired by provocative experiments featuring single molecules conducting current between two nearby electrodes (leads).[29,30] The integrity of the molecules under the influence of the immense applied electric field strengths on the order of 1 V nm^{-1}, carrying currents as much as 1 μA, has often been questioned, resulting in attempts to measure truly molecularly derived signals. Initially, this was achieved through measurement of the quantum mechanical Kondo effect on the conducting material,[31] but later efforts have concentrated on the measurement of the molecular vibrational spectrum using revitalized inelastic electron tunneling spectroscopy (IETS).[32,33] As IETS provides more high-resolution information concerning molecular conductivity than does any other available technique, it offers many advantages for the testing and verification of computational approaches such as gDFTB. Very little high-resolution information is experimentally available concerning the atomic structure of molecule−metal junctions, however, and it is in this area that computationally efficient approaches such as DFTB may prove to be very useful. It is generally assumed that actual junction structures consist of random, fluctuating surfaces with statistically oriented molecules and environments, a scenario that a method as efficient as DFTB could perhaps one day model. However, modelers usually assume interfaces with simple structures such as that depicted in Figure 1. This figure shows how a chemisorbed 1,4-benzenedithiol molecule may be attached to two parallel pure Au(111) surfaces. While there is no reason to believe that high-symmetry structures form in molecular junctions, calculations based upon this assumption
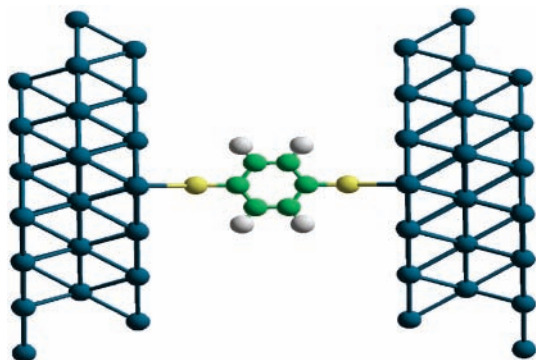
5694 *J. Phys. Chem. A, Vol. 111, No. 26, 2007*

Reimers et al.

Figure 1. The type of crude depiction of two metal electrodes (leads) spanned by a single molecule; in this case, two Au(111) surfaces are spanned by a chemisorbed 1,4-benzenedithiol (SC_6H_4S) molecule.

have been very successful in describing results from molecular electronics experiments. How can this be?

The Green's Function DFTB Method gDFTB

Early models for the steady-state conductivity of single molecules were based on the Landauer−Büttiker Green's function scattering theory for coherent elastic electron transport.[34−36] These were presented in their most developed forms by Mujica and Ratner[37,38] and by Datta,[2,39] formalisms that we have shown to be equivalent.[40] However, a more general formalism has also been developed based on the Meir−Wingreen equation[41] that can include all nonequilibrium effects, high nonequilibrium temperatures, and electron−phonon scattering, a formalism that forms the basis of the gDFTB method.[1−5] In the low-temperature low-voltage limit, this generalized approach reduces to the simpler one, with the exception that not only the coherent elastic term I_{el} emerges but, in addition, closely related inelastic components I_q

$$I = I_{el} + \sum_q I_q = \frac{2e}{h} \int_{\mu_R}^{\mu_L} g\, dE + \frac{2e}{h} \sum_q \int_{\mu_R}^{\mu_L} g_q\, dE \quad (7)$$

with

$$g = \text{Tr}[\Gamma_L G^r \Gamma_R G^a] = \text{Tr}[A_L^* \Gamma_R] \quad (8)$$

and

$$g_q = \text{Tr}[\Gamma_L G^r \alpha_q \tilde{G}^r \tilde{\Gamma}_R \tilde{G}^a \alpha_q G^a] = \text{Tr}[A_L^* \alpha_q \tilde{A}_R \alpha_q] \quad (9)$$

In these equations, I is the total current, the chemical potentials of the two electrodes (named L and R) differ by $\mu_L - \mu_R =$ the applied voltage V, E is the energy of the injected charge carrier, "~" indicates evaluation using the energy $E - \omega_q$ of the ejected charge carrier after excitation of molecular normal vibrational mode q at frequency ω_q, $G^r = (ES_M - \Sigma_L - \Sigma_R - H_M)^{-1}$ is the retarded Green's function of the molecule obtained from the one-particle molecular electronic Hamiltonian operator H as described below, G^a is the corresponding advanced Green's function $G^a = (G^r)^\dagger$. Also, the electron−phonon coupling constants involving motion along the dimensionless normal coordinate Q_q are given by

$$\alpha_q = \frac{\partial H_M}{\partial Q_q} - \frac{\partial S_M}{\partial Q_q} S_M^{-1} H_M - H_M S_M^{-1} \frac{\partial S_M}{\partial Q_q} \quad (10)$$

while S_M is the molecular atomic orbital overlap matrix, and Γ_L and Γ_R are the imaginary components of the self-energies

Σ_L and Σ_R depicting the interactions of the molecule with the L and R electrodes

$$\Sigma_L = J_L^\dagger G_L J_L \quad \Sigma_R = J_R^\dagger G_R J_R \quad (11)$$

where H_M, $G_L = (ES_L - H_L)^{-1}$, $G_R = (ES_R - H_R)^{-1}$, J_L, and J_R are obtained by partitioning the total Hamiltonian from a DFTB calculation on an large molecular complex containing the molecule and a (in principle, large) number of atoms representing the L and R electrodes

$$H = \begin{bmatrix} H_L & J_L^\dagger & 0 \\ J_L & H_M & J_R \\ 0 & J_R^\dagger & H_R \end{bmatrix} \quad (12)$$

Note, however, that such DFTB calculations need to be performed self-consistently, including the effects of the self-energies explicitly, as these modify the effective molecular electronic Hamiltonian. The electron−phonon (vibronic) coupling constants α_q are also evaluated using DFTB to deduce the normal modes and vibrational frequencies of the molecule and, hence, the appropriate derivatives of H_M. The equations can be simplified further[11] by neglecting the ejection matrices at energy E rather than at $E - \omega_q$, resulting in the approximation

$$G^r \alpha_q \tilde{G}^r \approx \frac{\partial G^r}{\partial Q_q} \quad (13)$$

that leads to the qualitatively useful form[42]

$$g_q \approx \text{Tr}\left[\Gamma_L \frac{\partial G^r}{\partial Q_q} \Gamma_R \frac{\partial G^a}{\partial Q_q}\right] \quad (14)$$

The Need to Treat Large Nanosized Systems

Central to the application of Green's function approaches is its handling of the open boundary conditions. The effects of the semi-infinite contacts are treated using two non-Hermitian, nonlocal, energy-dependent functionals called self-energies. These are computed from the bulk properties of the contacts and map the open infinite energy levels of the contacts onto a smaller central region, a region that includes the bridging molecule. The Hamiltonian of the central region becomes the original single-particle Hamiltonian plus the self-energies, thus gaining an imaginary non-Hermitian component. The inverse of the imaginary part of the resulting eigenvalues represents the lifetime of an electron in the central region before it is transferred to one of the electrodes. After this mapping is done, we do not need any more information about the contacts, and all of the matrices involved in the calculation of the current have the size of the central region only. However, finding the best partitioning of the whole systems into regions depicting the two contacts and the central region is an issue.

Many systems studied experimentally involve sulfur linkages between molecules and gold surfaces, linkages that are stronger than the bonds between the gold surface atoms. Hence, the obvious choice of partitioning the system at the gold−sulfur junctions may not be a good one. As a result, quantitative calculations consider "extended molecules" that include not only the organic component but also significant numbers of atoms from the junction regions of the electrodes. As the size of the explicitly treated quantum system grows, the Green's function approaches become more accurate, giving the exact current in the limit of infinitely sized extended molecules.
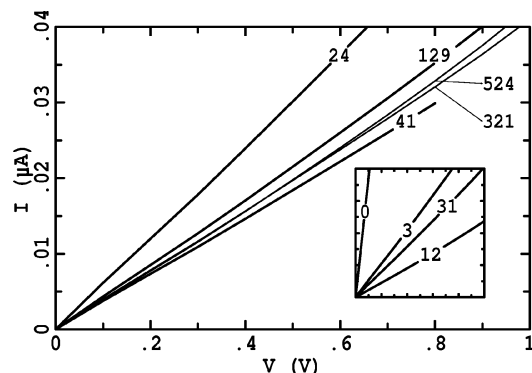
DFTB for Molecular Electronics

J. Phys. Chem. A, Vol. 111, No. 26, 2007 **5695**

Figure 2. Convergence of the INDO-calculated current−voltage curves[46] for 1,4-benzenedithiol chemisorbed between two Au(111) surfaces with respect to the total number of atoms in each electrode (three Au atoms per electrode in the extended molecule); the inset shows convergence with respect to the number of atoms of each cluster in the extended molecule for 321 atom electrodes.

It is hence important to determine how large the extended molecule must be in order to calculate converged currents. First, we investigated[43] the behavior of atomistic systems using classical electrostatics and using the semiempirical Hartree−Fock-based intermediate neglect of differential overlap[44,45] (INDO) quantum chemical technique. This study demonstrated that very large systems involving hundreds to thousands of atoms are required in order to establish the validity of Gauss's Law of classical continuum electrostatics, image−charge approaches to modeling the interaction of electrode interfaces with charge-polarized molecules, and standard relationships involving capacitance. Such results would also be expected to apply to the continuity of properties across the chosen junction surfaces in Green's function calculations. Next, we investigated[46] Green's function calculations of coherent through-molecule transport using INDO, obtaining similar results. Calculations[46] depicting the convergence of calculated current−voltage curves for chemisorbed 1,4-benzenedithiol between two gold electrodes are shown in Figure 2, where it is demonstrated that on the order 300 atoms are required in each electrode, and of these 300 atoms, on the order 30 must be included in the extended molecule.

Applications of standard DFT to molecular electronics have been hampered by the high level of computational resources required. Often only 1−3 metal atoms are included in calculations. As single-molecule conductivity is, at its core, a molecular property, such calculations have been very useful in understanding basic principles, but they cannot be used in quantitative calculations. Single-molecule conductivity is, in reality, a nanoscale phenomenon; however, its details are controlled by the interface structure and the properties of the electrode contacts. DFT-based computational methods that focus on quantitative accuracy as a desired goal, such as TRANSI-ESTA,[6,7] use much larger samples to represent the electrodes, typically on the order 30 atoms each, coupled with analytical boundary-matching techniques to accelerate convergence. Nevertheless, explicit calculations using samples of the order required to converge the nanoscopic properties of the included gold atoms remain impractical.

This led to the initial vision for the development of gDFTB; DFTB is as computationally efficient as is INDO, yet it should, in principle, be much more accurate for key energy differences while allowing for geometry optimization, device structure investigations, and calculations of phonon structure. It could facilitate the solution of problems not practical by DFT methods such as investigation of sample size convergence, molecular

dynamics calculations of arbitrary thermal structures, heat dissipation in the molecule and junction region due to current flow, and so forth. Indeed, initial studies have indicated that gDFTB can be successfully applied to study large systems,[13] inelastic scattering processes,[12] and device heating.[5]

Systematic Failures of Conventional DFT in Molecular Electronics Applications

In principle, gDFTB could have advantages over the use of conventional DFT in molecular electronics applications, owing to the number of significant limitations known to be associated with modern density functionals. These include[47] poor treatment of dispersive forces, covalent bond breakage, systems involving partial electron removal, and conjugated π systems.

First, dispersive forces are very important for the determination of the geometrical structure of interfaces, being the primary contributor to physisorptive processes including the strong π-stacking interactions that can occur between gold and aromatic molecules,[48] the interactions of nitrogen bases with gold,[49] and contributions along with covalent bonding to thiol−gold interactions.[50] While these forces are treated empirically and sporadically by DFT,[51] they are also excluded from the basic DFTB Hamiltonian. However, while the DFTB formalism (eq 1−14) has been extended to explicitly include these forces,[52] allowing, for example, their inclusion into protein force fields,[53] parametrization of gold has not been completed. This aspect provides a significant avenue for further development.

Second, we note that, in general, covalent bond breakage is treated poorly by modern DFT functionals, with their poor description of long-range electron correlation leading to contamination of supposedly radical-like reaction products with ionic-like structures.[54−58] This failure has immediate consequences for the determination of realistic strained electrode−molecule junction structures as dynamic bond breaking and forming processes are likely to be important. However, it has more profound effects owing to the way in which Green's function-based methods perceive the current carrying process.[17] In effect, they perceive conduction as occurring between the two macroscopic contacts through tunneling. All that is important is the tunneling probability, effectively obtained from the calculated energy gap between the electrode-localized tunneling orbitals. The process by which this energy gap arises is irrelevant; it could be via direct through-space interactions of the electrodes or via superexchange[5] through molecule-assisted pathways. Viewed in this way, through-molecule conduction is analogous to through-space conduction between two electrodes with broken interelectrode covalent bonds, allowing errors associated with covalent bond breakage to enter calculations in a profound way. Formally correct solutions to the Kohn−Sham equation of DFT can only be obtained under highly restricted conditions,[59] though computational codes will always return a solution. Covalent bond breakage is an open-shell problem for which valid solutions may be obtained using spin-unrestricted means if just one bond is involved,[59] a situation not typical in molecular electronics applications. Inappropriate application of the Kohn−Sham theorem leads to overestimation by possibly an excess of excited-state energies, energies interpreted by Green's function codes as depicting the strength of tunneling, leading to gross overestimation of the conductivity.

An illustrative example of the principle is shown in Figure 3 in which the four orbital energy levels near the Fermi energy for two Au_3 clusters held in parallel triangular faces a distance R apart are plotted as the two systems are pulled apart. This is an open-shell problem involving two electrons in four orbitals,
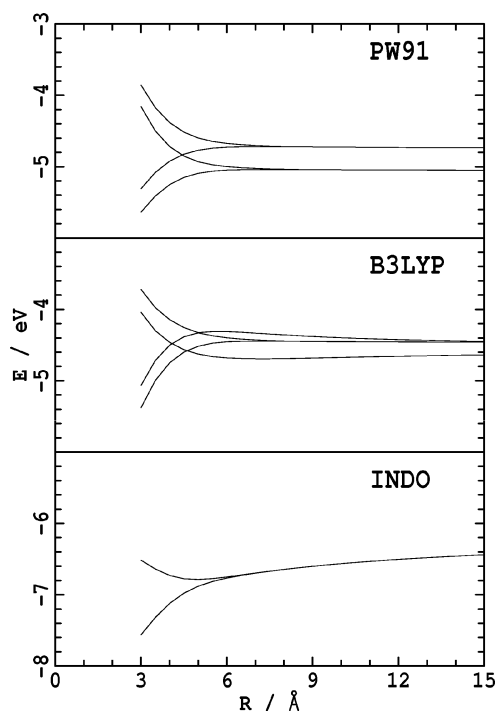
Figure 3. The four orbitals near the Fermi energy for two Au_3 triangles held with faces parallel at a distance R apart, as calculated using the PW91 GGA, the B3LYP hybrid density functional, and INDO using spin-restricted open-shell techniques; only INDO correctly depicts two pairs of degenerate orbitals.

a problem that may be solved easily using wave function-based approaches such as INDO, yielding two degenerate pairs of orbitals that smoothly become 4-fold degenerate asymptotically, as shown in the figure.[17] However, no valid solution can be obtained for the Kohn–Sham equation in this case, and the orbital eigenvalues obtained[17] using PW91,[60] a popular generalized gradient approximations (GGA) density functional, show incorrect asymptotic properties with a residual, artifactual, band gap appearing between degenerate orbital pairs. Very much worse[17] results are obtained using the hybrid density functional B3LYP,[61] however, with the eigenvalues asymptotically falling into groups of 1 and 3 orbitals.

As a result, it is concluded that hybrid density functionals such as B3LYP should not be used in molecular electronics applications. Also, as the local density approximation (LDA) in DFT provides realistic treatments of most metal electrodes but gives a very poor description of the molecular component; its usefulness in molecular electronics calculations is also very limited. Hence, of the types of density functionals in common use, only GGAs may meaningfully be used, and as Figure 3 indicates, this use still requires caution. Only hybrid functionals, however, include the long-range exchange interactions that are often critical in electron-transfer problems. Hence, while the development of improved density functionals is a priority, there is scope for methods such as DFTB that do not suffer from the covalent bond breakage anomaly to be very useful in molecular electronics research.

The third limitation of conventional DFT is manifest for partial charge separation. In this scenario, the electron is removed a long distance from its atom but not removed completely from the system. As modern density functionals employ independent exchange and correlation functionals, contributions at large distance to the energy that should cancel do not,[62] with the result that the electron sees itself, the so-called self-interaction energy error.[62–67] Practically, this results

in low energies for charge-transfer states, a type of state that can contribute to through-molecule conductivity, and an incorrectly positioned molecular highest-occupied molecular energy (HOMO) level that is typically too high in energy by 3–4 eV. In molecular electronics applications, this leads to huge errors in the lineup of the orbital bands of the electrodes and the molecule,[48,68] an effect that should, at first thought, render unrealistic most through-molecule conductance calculations performed using DFT. An example of this effect is provided in Figure 4 where results for the phenylthiol molecule, its deprotonated radical and anion forms, its chemisorbate on Au(111), and the clean Au(111) surface are shown; in this case the band lineup error is 3.4 eV. However, as the figure indicates, charge injection into the molecule dramatically shifts the energy levels and thus causes the bands to properly align; instead of catastrophic failure of the method, only quantitative inadequacies in the description of charge flow and polarization thus result. In principle, DFTB could overcome this error as it does not facilitate self-interaction errors.

Last, we consider limitations of standard DFT in treating conjugated π systems. Many molecules used in molecular electronics applications, especially the highly conductive ones, such as 1,4-benzenedithiol, are of this type. Molecular conduction involves partial oxidation or reduction processes of the molecule, processes whose energies are identified in single-particle implementations of Green's function kinetics theories with molecular orbital energy differences. While such an identification follows naturally from Hartree–Fock-based approaches through application of Koopmans's theorem, in DFT, the calculated orbital energy differences actually form an order-zero approximation to the much smaller energies associated with optical transitions.[69] This disparity leads to an error of 5.6 eV for the calculated band gap of phenylthiol, the molecule used as an example in Figure 4.[68] Unfortunately, DFTB is also subject to errors of this type,[70] but improvements that maintain a reasonable level of computational efficiency involving application of the GW method are being developed.[71]

For standard DFT, the interplay between the self-interaction correction (HOMO error) and the undesired physical interpretation of the band gap is complex. Fortunately, the two errors cancel to some extent for the band lineup of the molecular lowest-energy unoccupied molecular orbital (LUMO), giving an error of just $5.6 - 3.4 = 2.2$ eV for the phenylthiol example used in Figure 4.[48,68] However, as the self-interaction error also results in significant underestimation of the actual excited-state optical transition energies, both effects reinforce each other in making molecules appear metal-like. Polyacetylene, for example, is predicted by modern density functionals to have a ground state of at least triplet spin multiplicity rather than being a wide-band-gap semiconductor,[72] with associated errors in calculated polarizabilities for the actual closed-shell ground state.[73] Porphyrin and chlorophyll molecules, ubiquitous for their roles in naturally occurring systems involving through-molecule conduction, are also poorly described.[72,74] Many new functionals have been designed to overcome these problems, but for porphyrins and chlorophylls, we find that only one, CAM-B3LYP,[66] provides realistic results.[75] While this functional is a hybrid functional embodying a component of long-range exchange, the means by which it is included may also reduce the magnitude of its errors associated with covalent bond breakage.

In conclusion, we see that standard DFT approaches using currently available functionals embody a significant number of fundamental limitations when it comes to quantitative applications in molecular electronics. The simplifications introduced
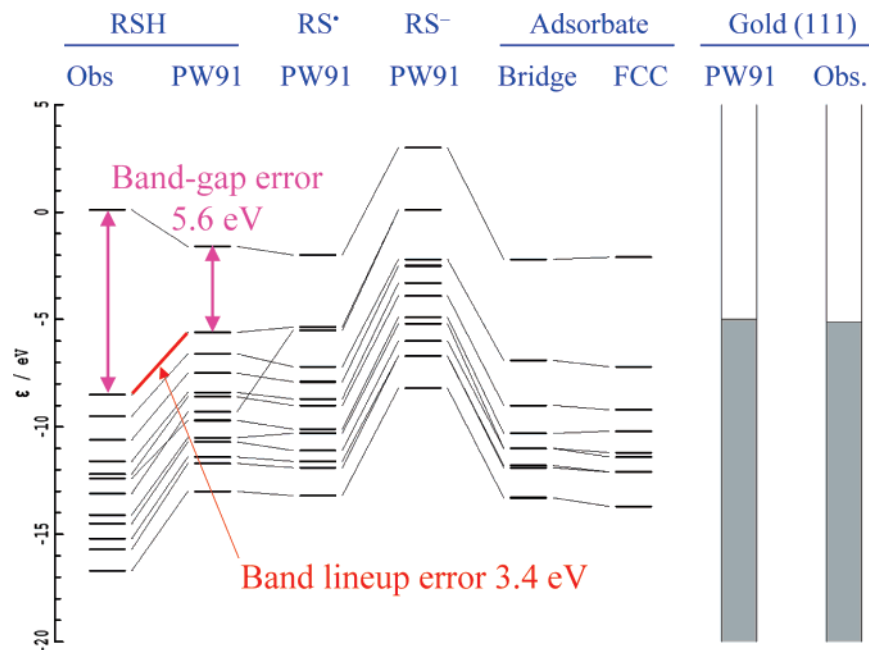
DFTB for Molecular Electronics

J. Phys. Chem. A, Vol. 111, No. 26, 2007 **5697**

Figure 4. Calculated[68] (using the PW91 GGA) and observed orbital energy levels ϵ or orbital bands for phenylthiol RSH, the phenylthiol radical RS·, the phenylthiolate anion RS$^-$, chemisorbed RS on bridge and fcc surface sites, and the clean unreconstructed Au(111) surface, highlighting the band gap and HOMO band lineup errors of DFT.

in the design of DFTB not only lead to its increased computational efficiency but also to the overcoming of some of these problems, with the potential to overcome others.

Preliminary DFTB Results for the Prediction of Interface Geometries

While a major aim is to model high-temperature current-carrying irregular electrode−molecule interfaces, detailed assessment of the accuracy of DFTB is best obtained from calculations on simple systems such as dilute alkanethiol monolayers on gold (111). A desirable result would be for DFTB to correctly predict experimental observations, although, as DFTB is obtained as an approximation to DFT, if DFT and experiment differ, then it is likely that DFTB mimics DFT more than it mimics experiment. The binding geometry of alkylthiol molecules chemisorbed (with terminal proton loss from sulfur during the adsorption process) on gold surfaces has received considerable attention in the literature,[76−90] without definitive conclusions being reached. At issue is whether or not thiol monolayers reconstruct the surface, as well as the detailed propensities for binding at different surface sites.

The most detailed information available experimentally indicates that sulfur atoms sit vertically above gold atoms on the surface,[91,92] with evidence suggesting that no reconstruction is involved. In addition, however, self-assembled monolayers have recently been observed that involve horizontal binding to gold adatoms sitting above the usual surface.[93] DFT calculations performed on flat Au(111) surfaces,[68,84−86,88−90] however, indicate that binding to bridge sites, fcc hollow sites, and sites in between these two classic locations should be very much stronger than that atop of gold atoms. Also, DFT calculations first led to the prediction that thiols bind to adatoms; however, the binding geometry is calculated to be vertically aligned[94] as opposed to the observed horizontal alignment.[93] Hence, while DFT calculations and experiment lead to the notion that many styles of binding are feasible, they differ significantly in quantitative details that are highly relevant to the operation of molecular electronic devices.

TABLE 1: Calculated Relative Energies ΔE (kcal mol^{-1}) and Bond Lengths (Å) between Gold (Au), Sulfur (S), Bridge Carbon (C), *ortho*-Carbon (C$_o$), *meta*-Carbon (C$_m$), and *para*-Carbon (C$_p$) Atoms for Thiophenyl Radicals C$_6$H$_5$S on Au(111) Constrained Such That the CS Bond Is Normal to the Surface

structure	method	ΔE	Au−S	S−C	C−C$_o$	C$_o$−C$_m$	C$_m$−C$_p$
fcc	PW91	[0]	2.48	1.79	1.40	1.40	1.40
	DFTB	[0]	2.70	1.78	1.41	1.39	1.40
hcp	PW91	0.8	2.52	1.78	1.40	1.40	1.40
	DFTB	3.0	2.49	1.79	1.41	1.39	1.40
bridge	PW91	1.5	2.50	1.78	1.40	1.39	1.40
	DFTB	6.4	2.54	1.79	1.40	1.39	1.40
top	PW91	11.6	2.57	1.74	1.41	1.39	1.40
	DFTB	25.5	2.91	1.77	1.41	1.39	1.40

DFTB predicts[12] that chemisorption of alkanethiols above the top sites of unreconstructed surfaces leads to a local-minimum configuration, unlike results from conventional DFT.[68,84−86,88−90] However, as this structure could be the experimentally observed one,[91,92] we have exploited it in practical calculations of IETS measurements.[12] Unfortunately, no comprehensive study of the surface topology for thiol chemisorbates on gold has been performed. Some preliminary results for the chemisorption of phenylthiol on gold (111) are given in Table 1, however, where they are compared with results obtained[68] using the PW91[60] density functional. Note that all structures described in the table have their CS vectors oriented vertically above the surface, configurations that are typically higher in energy than bent structures but ones that may be more relevant to molecular electronics applications. These structures involve the sulfur atom binding above fcc hollow, hcp hollow, bridge, and top sites on the (111) surface. Both PW91 and DFTB predict that the site interaction energies increase in the order fcc < hcp < bridge < top, but the calculated energy differences vary considerably. In particular, the top site is a local-minimum structure for DFTB at a relative energy of 11.6 kcal mol^{-1} compared to the fcc site, but for PW91, it is a saddle point removed by 25.5 kcal mol^{-1}. The bond lengths calculated by both methods are also shown in Table 1. Very good agreement is found between the PW91- and DFTB-calculated C−C and C−S bond lengths, but

there is considerable variation for the Au−S ones. These results indicate that DFTB shows promise as a tool for evaluating complex interfaces, but much more calibration and evaluation is required.

Experimental Demonstrations of the Role of Molecular Symmetry in Molecular Conduction

Owing to the lack of detailed information contained in current−voltage characteristics depicting coherent charge transport through molecules, the strong interactions between electrodes and thiol-bound molecules, and perceived irregularities in junction structures, there has traditionally not been much concern shown for the role of molecular symmetry in determining conduction. Molecular symmetry, is, however, a key factor determining molecular spectroscopic properties and intramolecular electron-transport properties,[95] and hence, a significant role in steady-state conductivity can be anticipated.

The first experimental results providing specific symmetry information were obtained using IETS to measure molecular vibrational frequencies through detection of inelastic charge-transport processes in molecular electronics.[32,33] Initially, there appeared to be no selection rules operative, with modes of all symmetry classes being observed to scatter transporting charges. High amplitudes for scattering by certain classes of modes were observed, however, and propensity rules[11,42] became required in order to qualitatively interpret observed results. While such rules must clearly originate from molecular processes, their nature and the effect of the environment on lowering the in vitro symmetry of the conducting molecule remained to be determined.

Implementing Symmetry in DFTB

Enhanced Computational Stability and Efficiency. The standard DFTB program package does not detect or utilize molecular symmetry in its function. While exploitation of symmetry was essential in the early years of quantum chemistry, owing to the significant cost savings that occur for the study of symmetric molecules, modern programs such as DFTB that are designed for use in asymmetric biological applications have not found their inclusion warranted. To allow gDFTB to be used to discover the role of molecular symmetry in single-molecule conduction, extensive implementation of molecular symmetry within DFTB is required, however. Analysis of symmetry information remains generally important in chemical applications of DFTB.

Abelian point group symmetry was implemented into DFTB using procedures developed[96] for multireference configuration−interaction treatments of excited states using INDO. The symmetry point group operators of the system were determined. A symmetry transformation matrix was then constructed, allowing the atomic orbital basis functions to be combined into symmetry-adapted linear combinations. The DFTB Hamiltonian and overlap operators were then generated as usual but were transformed into the symmetry-adapted atomic orbital basis before diagonalization. Each symmetry block was then transformed independently, and the resultant eigenvalues and eigenvectors were labeled by their symmetry before being back-transformed and sorted so as to mimic the results obtained by the usual symmetry-ignoring diagonalization routines. The self-consistent charge loop of the SCC-DFTB was then executed as normal, stopping when converged wave functions were obtained. For molecules such as deprotonated 1,4-benzenedithiol that belong to the D_{2h} point group, this procedure resulted in an order-16 decrease in the computer time required for matrix diagonalization, the most expensive aspect of DFTB calculations.

Hessian matrices for use in determining the normal modes of vibration and their frequencies were obtained using an analogous procedure, forming the usual symmetry-adapted Hessian matrix and then transforming it into symmetry-adapted Cartesian coordinates. The original Hessian matrix was obtained by numerical differentiation in terms of Cartesian coordinates of analytically derived atomic force vectors, however, an approach that did not make use of molecular symmetry. Alternative use of symmetry-adapted Cartesian coordinates during these numerical differentiation steps would yield another order-16-fold decrease in the time required to calculate the vibrational frequencies for a molecule of D_{2h} symmetry. Combined with the already established savings in evaluating the required forces, this would deliver a net order-64-fold decrease in the required computer time.

The implementation of symmetry in DFTB not only provides key information and reduces the computational time, it also significantly increases numerical stability. The additional computer time required by non-symmetry-adapted approaches can be considered as providing the calculation of the much larger number of matrix elements that connect basis vectors in different symmetry blocks, matrix elements whose value should be precisely zero. Numerical imprecision in the integration routines used inside DFTB to calculate matrix elements causes the calculated numbers to differ from zero, however, leading to the development by Morokuma[97] of alternative means of evaluating the DFTB core operations. While any particular evaluation of these errors leads to small and presumably negligible quantities, their continued feedback into the self-consistent charge loop via their manifestation through a deduced molecular charge distribution that does not conform to that required by the point group symmetry can lead to their exponential amplification if the Lyapunov exponent[98,99] for their propagation indicates that the SCC-DFTB equations are unstable. We find this to be a common occurrence for the problems of current interest. In many applications, this type of instability may be viewed as a helpful feature, as it will allow a low-energy structure to be found at the expense of high-energy transition states. However, for the understanding of molecular symmetry, its role, and function, such instabilities prevent the desired information from being obtained. This makes the proper implementation of molecular symmetry within DFTB essential for the practical calculation of meaningful quantities.

Finally, we note that the vibronic couplings α_q required in gDFTB are evaluated numerically using eq 10 by displacing the molecular coordinates in the full symmetry-adapted normal modes of vibration, thus taking full advantage of molecular symmetry during this expensive operation.

The Molecular Conductance Point Group. Molecular conduction is a nonequilibrium process, and hence, it is not immediately clear how molecular point group symmetry, an equilibrium molecular property, could influence it. The non-equilibrium nature of the process is fully captured within the gDFTB approach, and examination of eqs 8 and 9 reveals the elements of symmetry that are lost or retained. For simplicity, we assume that the molecule bridges the two electrodes symmetrically, as depicted in Figure 1, so that the self-energies Σ_L and Σ_R and their imaginary components Γ_L and Γ_R are related by end-to-end symmetry operators of the zero-voltage equilibrium system. As a result, the Green's functions G^r and G^a display the full system symmetry, as must α_q. However, from eqs 11

DFTB for Molecular Electronics

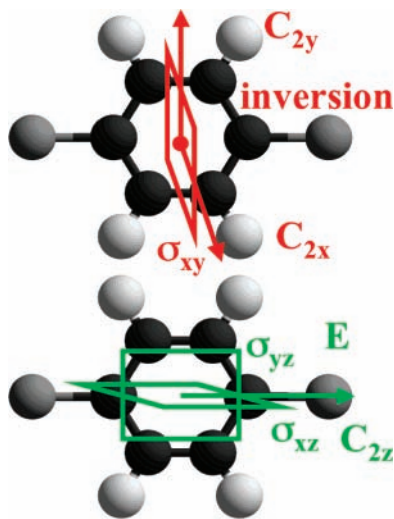*J. Phys. Chem. A, Vol. 111, No. 26, 2007* **5699**

Figure 5. The D_{2h} symmetry operators that define the geometric point-group-chemisorbed 1,4-benzenedithiol (SC_6H_4S) are separated into those (red) depicting end-to-end symmetry that are eliminated by the current flow and those (green) that are preserved, defining the molecular conductance point group C_{2v}; Reproduced from ref 13 with permission of *The American Institute of Physics.*

and 12, it is clear that Σ_L and Γ_L display only the common symmetry elements of the L electrode (as embodied within G_L) and the L electrode−molecule junction (as embodied within J_L), and this is similar for the R electrode. These common operators define the conductance point group of the system, a rigorous quantity that describes the symmetry properties of single-molecule conduction.[13]

While the conductance point group is rigorous in its definition, it could be thought to be irrelevant in its application to experimental problems as any asymmetry in the two junctions, including the electrode shapes, binding sites, and so forth, would reduce the conductance point group to the null group C_1, eliminating any role for symmetry. However, solution of the gDFTB equations indicates quantitatively accurate calculations can be performed, working in the framework of a (commonly) approximate point group, the molecular conductance point group, defined in terms of only the properties of the bridging molecule.[13] This point group is obtained from the point group of the isolated chemisorbed molecule, removing any operators that depict end-to-end symmetry. An example is shown in Figure 5 for 1,4-benzenedithiol after its chemisorptive proton loss; the molecular symmetry is d_{2h}, but loss of end-to-end symmetry produces a molecular conductance point group of C_{2v} symmetry.[13] Note that lowercase symmetry descriptors are used to depict molecular symmetry, while uppercase descriptors are used to depict the molecular conductance point group symmetry.

Qualitative Results

The Assignment of Observed IETS. The gDFTB formalism has been shown[12] to provide a qualitatively realistic description of the observed[32] IETS of octanedithiol chemisorbed between conducting contacts. Since then, the gDFTB code has been symmetry enabled, allowing characterization through symmetry assignment of the observed data. The low-resolution calculated[12] and observed[32] IETS are shown in Figure 6, along with symmetry assignments of the calculated high-resolution IETS made using the recent symmetry-enabled gDFTB program.[11] While the agreement found between observed and calculated intensities is only qualitative, it indicates that gDFTB may

fruitfully be used to interpret detailed molecular characteristics of single-molecule conduction. Totally symmetric (a_g) modes dominate the conduction, as expected,[11,42] but other modes are also active. Previous enhanced assignments in terms of mode types have previously been detailed. Further, measurements of the IETS of related alkanedithiols have also been measured,[33] providing starkly different intensity patterns, a feature qualitatively interpretable by our IETS calculations,[12] as they indicate that the proximity of organic atoms to atoms from the contacts significantly modifies calculated intensities. These results highlight the need for the determination of more realistic, thermally averaged geometries for use in quantitative IETS simulations.

The Nature of Through-Molecule Coherent and Incoherent Steady-State Electron Transport. In this application, we harness the power of DFTB not to provide quantitatively accurate results on large systems but rather as a tool that returns results of calculations in real time to facilitate identification of the roles of all of the quantities that appear in the Green's functions equations. We hence choose model systems containing only 2−3 gold atoms representing each electrode and search for ways of rewriting eqs 8 and 9 so that they take on simple forms that provide physical insight into the processes controlling elastic and inelastic charge transport through molecules. A large number of approaches have been used, of which, four have been described,[11,14] each being useful in exposing one of the myriad of aspects that control through-molecule conduction. We shall consider two of these approaches only.

The first approach was inspired by the physical insight of Troisi and Ratner[42] that the matrices Γ are sparse, as only a few of the orbitals (on the sulfur atoms) of the molecule overlap with the metals. We showed that under the assumption of a single-orbital contact, the Γ matrices have unit rank.[14] Rewriting eqs 8 and 9 in the bases of the eigenvectors of these matrices thus provides dramatic simplification to the gDFTB equations. For 1,4-benzenedithiol chemisorbed between two gold electrodes, only 15 eigenvalues of Γ_L and Γ_R are nonzero; note that these two sets of eigenvalues are identical as the two junctions are assumed to be symmetrically related. Of these, only 4 are actually significant; the most dominant two are of A_1 symmetry, providing conduction through a channel of σ symmetry, and B_1 symmetry, providing conduction through a channel of π symmetry. The energy dependence of these junction channel eigenvalues is given in Figure 7 and is quite weak, with the A_1 channel being 10 times more conducive to carrying current than its B_1 counterpart.

The elastic current from eq 8 is obtained from these junction channel, with the molecular Green's function matrix elements acting to couple together the incoming and outgoing waves. If the junctions dominate the conductivity, then the transmission function $g(E)$ will be dominated by the A_1 channels at all energies. Also shown in Figure 7, however, are the two most influential eigenvalues of g, the largest ones of A_1 and B_1 symmetry. At energies near the Fermi energy (−4.8 eV) in the region that dominates low-voltage conductivity, elastic scattering through the B_1 channel is found to dominate, however, indicating that the properties of the molecule, as manifested through its Green's function matrix elements, have over-ridden the junctions' preference for A_1 transmission. This occurs, of course, because the molecule is a much better π conductor than a σ conductor; at energies away from the Fermi energy amidst the σ and σ^* orbital bands, the system does indeed prefer to conduct through its A_1 channel, but this is not a relevant process at attainable energies.

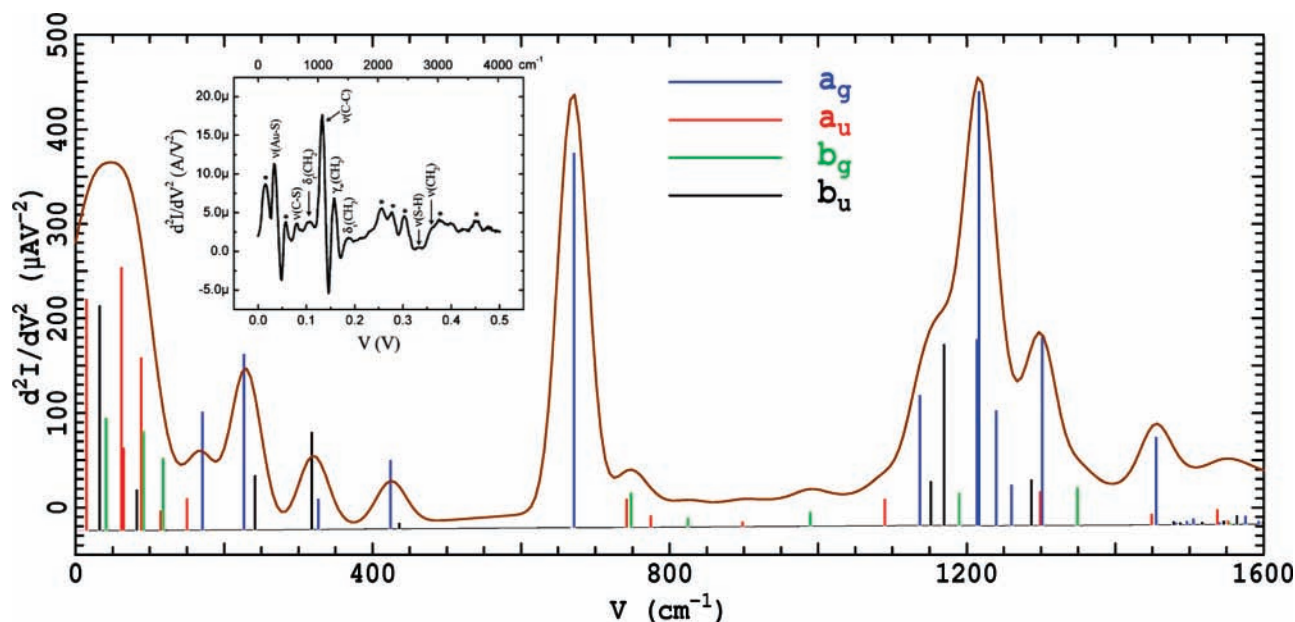**Figure 6.** Low-resolution and high-resolution IETS of octanedithiol chemisorbed on gold electrodes, as calculated[12] using gDFTB with the inclusion of subsequent symmetry assignments in terms of the c_{2h} molecular point group; the inset shows the observed IETS of Wang et al.[32] for comparison.
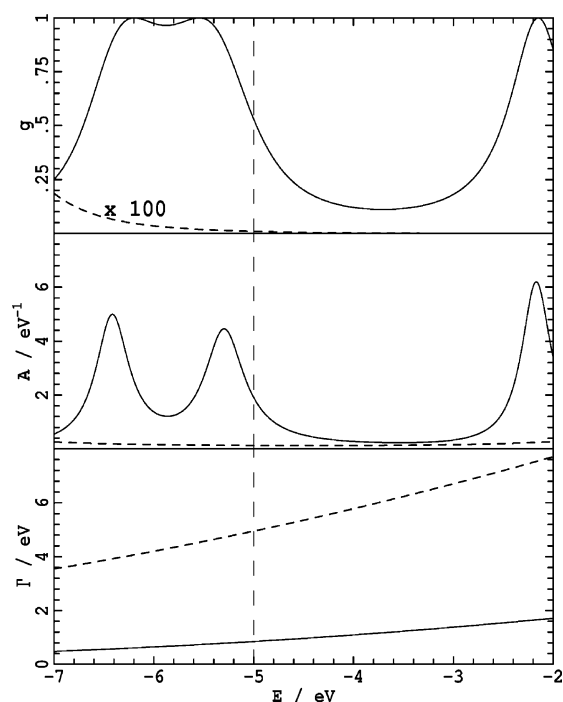

Figure 7. Energy dependence of the dominant eigenvalues of A_1 (σ, dashed) and B_1 (π, solid) symmetry of $\Gamma_L(E) = \Gamma_R(E)$ and $A_L(E) = \tilde{A}_R(E + \omega_q)$ as well as those for the elastic transmission $g(E)$.

Figure 8. Dominate eigenvectors of A_1 (σ) and B_1 (π) symmetry of $A_L(E) = \tilde{A}_R(E + \omega_q)$ that form the incoming and outgoing channels and the vibrational modes that most strongly couple these together to produce inelastic scattering; a_g modes are in-plane, totally symmetric vibrations, while b_{3u} and b_{2u} modes are out-of-plane modes that have B_1 symmetry in the molecular conductance point group.

The second approach was inspired by the need to build molecular properties into the description at a fundamental level. It proceeds by diagonalizing the density-weighed couplings A_L and $\tilde{A}_R$ in order to build in the molecular orbital structure. Serendipitously, this approach also incorporates the Troisi–Rater simplification as the rank of the A matrices cannot exceed those of the Γ matrices as $A = G\Gamma G^a$. The energy dependence of the dominant eigenvalues of A_L are also shown in Figure 7. These eigenvalues peak near molecular orbital energy levels, and, hence demonstrate the dominant nature of the B_1 channels for processes occurring near the Fermi energy.

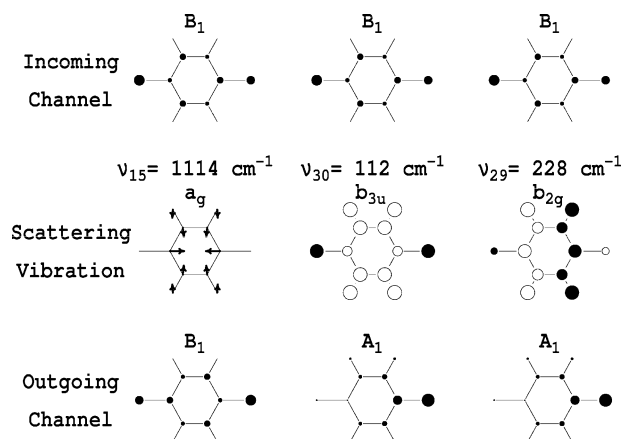This property is exploited in Figure 8 where the general principle controlling the propensities for the molecule to inelastically scatter conducting charges is described. The eigenvectors depicting charge carriers incoming and outgoing through the dominant A_1 and B_1 channels are described. Only vibrational modes of a_g symmetry may scatter carriers entering the dominant B_1 entry channel into the dominant B_1 exit channel,[11] and hence, these modes are the most intense ones in IETS. The form of the most intense calculated IETS vibration is also shown in the figure, its effect being to operate on the CS stretching modes as these are common to both the incoming and outgoing channel eigenvectors. Incoming charge carriers through the dominant B_1 entry channel may be scattered by both b_{3u} and b_{2g} modes into the secondary A_1 exit channel (and vice versa), allowing for out-of-plane modes to scatter transporting charges. As the figure shows, intense modes must modify the regions of the molecule that are in common with the entry and exit channels; in this case, the CS bonds are again prominent in the process. Strong interference between charges scattered in different regions of the molecule occurs, however.[11]

DFTB for Molecular Electronics

J. Phys. Chem. A, Vol. 111, No. 26, 2007 **5701**

Conclusions

The gDFTB method has been established and shown to provide a realistic qualitative description of elastic and inelastic charge transport through molecules, including molecular heating and other nonequilibrium effects. It is based on a powerful form of the NEGF theory for charge transport through mesoscopic structures and becomes formally exact in the limit of the treatment of infinite-sized samples. While the application of DFTB in this approach was initially motivated by the need for sufficient speed so that large systems could be treated at high temperature, DFTB has been shown to be effective in providing a simulation tool to help in the development of analytical models that seek to understand the basic properties of through-molecule conduction. Successes of the method, to date, include the ability to interpret and assign experimental IETS results and the identification of the role of molecular symmetry in determining conduction.

An important area that remains relatively unexplored is the ability of DFTB to predict realistic geometrical structures for metal–molecule interfaces, both at low temperature and at high temperature. Owing to the importance of dispersive forces in determining many metal–molecule interactions, the extension of the present DFTB model for gold to include dispersive interactions is a high priority. Detailed maps of gold–thiol potential energy surfaces are also required. All aspects of DFTB are relevant to its ability to quantitatively predict the properties of through-molecule conduction, and the accuracy to which DFTB can predict molecular band gaps and band alignments must also be established.

Symmetry has been implemented into the DFTB code. This allows not only symmetry properties to be deduced but also the exploitation of them to enhance computational efficiency and decrease numerical instability. In particular, the increase in numerical stability is an important feature that will facilitate practical chemical applications of DFTB in areas requiring accurate numerical differentiation of molecular properties, including potential energy surface production. These features will facilitate the widespread deployment of DFTB as a tool for chemical research.

References and Notes

(1) Keldysh, L. V. *Sov. Phys. JEPT* **1965**, *20*, 1018.

(2) Datta, S. *Electronic Transport in Mesoscopic Systems*; Cambridge University Press: Cambridge, U.K., 1997.

(3) Pecchia, A.; Di Carlo, A.; Gagliardi, A.; Sanna, S.; Frauenheim, T.; Gutierrez, R. *Nano Lett.* **2004**, *4*, 2109.

(4) Pecchia, A.; Di Carlo, A. *Rep. Prog. Phys.* **2004**, *67*, 1497.

(5) Jortner, J.; Nitzan, A.; Ratner, M. A. *Lecture Notes in Physics: Introducing Molecular Electronics*; Cuniberti, G., Fagas, G., Richter, K., Eds.; Springer: Berlin, Germany, 2005; Vol. 680; p 13.

(6) Brandbyge, M.; Mozos, J.-L.; Ordejon, P.; Taylor, J.; Stokbro, K. *Phys. Rev. B* **2002**, *65*, 165401.

(7) Sanchez-Portal, D.; Ordejon, P.; Artacho, E.; Soler, J. M. *Int. J. Quantum Chem.* **1997**, *65*, 453.

(8) Damle, P. S.; Ghosh, A. W.; Datta, S. *Phys. Rev. B* **2001**, *64*, 201403/1.

(9) Xue, Y.; Datta, S.; Ratner, M. A. *Chem. Phys.* **2002**, *281*, 151.

(10) Taylor, J.; Guo, H.; Wang, J. *Phys. Rev. B* **2001**, *63*, 245407.

(11) Gagliardi, A.; Solomon, G. C.; Pecchia, A.; Frauenheim, T.; Di Carlo, A.; Hush, N. S.; Reimers, J. R. *Phys. Rev. B* **2007**, in press.

(12) Solomon, G. C.; Gagliardi, A.; Pecchia, A.; Frauenheim, T.; Di Carlo, A.; Reimers, J. R.; Hush, N. S. *J. Chem. Phys.* **2006**, *124*, 094704.

(13) Solomon, G. C.; Gagliardi, A.; Pecchia, A.; Frauenheim, T.; Di Carlo, A.; Reimers, J. R.; Hush, N. S. *J. Chem. Phys.* **2006**, *125*, 184702.

(14) Solomon, G. C.; Gagliardi, A.; Pecchia, A.; Frauenheim, T.; Di Carlo, A.; Reimers, J. R.; Hush, N. S. *Nano Lett.* **2006**, *6*, 2431.

(15) Porezag, D.; Frauenheim, T.; Kohler, T.; Seifert, G.; Kaschner, R. *Phys. Rev. B* **1995**, *51*, 12947.

(16) Elstner, M.; Porezag, D.; Jugnickel, G.; Elsner, J.; Haugk, M.; Frauenheim, T.; Suhai, S.; Seifert, G. *Phys. Rev. B* **1998**, *58*, 7260.

(17) Solomon, G. C.; Reimers, J. R.; Hush, N. S. *J. Chem. Phys.* **2004**, *121*, 6615.

(18) Elstner, M.; Cui, Q.; Munih, P.; Kaxiras, E.; Frauenheim, T.; Karplus, M. *J. Comput. Chem.* **2003**, *24*, 565.

(19) Krueger, T.; Elstner, M.; Schiffels, P.; Frauenheim, T. *J. Chem. Phys.* **2005**, *122*, 114110.

(20) Niehaus, T. A.; Elstner, M.; Frauenheim, T.; Suhai, S. *J. Mol. Struct.: THEOCHEM* **2003**, *541*, 185.

(21) Shishkin, O. V.; Gorb, L.; Luzanov, A. V.; Elstner, M.; Suhai, S.; Leszczynski, J. *J. Mol. Struct.: THEOCHEM* **2003**, *625*, 295.

(22) Zhou, H. Y.; Tajkhorshid, E.; Frauenheim, T.; Suhai, S.; Elstner, M. *Chem. Phys.* **2002**, *277*, 91.

(23) Abdali, S.; Niehaus, T. A.; Jalkanen, K. J.; Cao, X.; Nafie, L. A.; Frauenheim, T.; Suhai, S.; Bohr, H. *Phys. Chem. Chem. Phys.* **2003**, *5*, 1295.

(24) Dolgonos, G.; Lukin, O.; Elstner, M.; Peslherbe, G. H.; Leszczynski, J. *J. Phys. Chem. A* **2006**, *110*, 9405.

(25) Porezag, G. D.; Pederson, M. R.; Frauenheim, T.; Koehler, T. *Phys. Rev. B* **1995**, *52*, 14963.

(26) Elstner, M.; Porezag, D.; Jungnickel, G.; Elstner, J.; Haugk, M.; Frauenheim, T.; Suhai, S.; Seifert, G. *Phys. Rev. B* **1998**, *58*, 7260.

(27) Aviram, A.; Ratner, M. A. *Chem. Phys. Lett.* **1974**, *29*, 277.

(28) Hush, N. S. *Ann. N.Y. Acad. Sci.* **2003**, *1006*, 1.

(29) Reed, M. A.; Zhou, C.; Muller, C. J.; Burgin, T. P.; Tour, J. M. *Science* **1997**, *278*, 252.

(30) Chen, J.; Reed, M. A.; Rawlett, A. M.; Tour, J. M. *Science* **1999**, *286*, 1550.

(31) Liang, W.; Shores, M. P.; Bockrath, M.; Long, J. R.; Park, H. *Nature* **2002**, *417*, 725.

(32) Wang, W.; Lee, T.; Kretzschmar, I.; Reed, M. A. *Nano Lett.* **2004**, *4*, 643.

(33) Kushmerick, J. G.; Lazorcik, J.; Patterson, C. H.; Shashidhar, R.; Seferos, D. S.; Bazan, G. C. *Nano Lett.* **2004**, *4*, 639.

(34) Landauer, R. *IBM J. Res. Dev.* **1957**, *1*, 223.

(35) Landauer, R. *Phys. Rev. A* **1981**, *85*, 91.

(36) Büttiker, M.; Imry, Y.; Landauer, R.; Pinhas, S. *Phys. Rev. B* **1985**, *31*, 6207.

(37) Mujica, V.; Kemp, M.; Roitberg, A.; Ratner, M. A. *J. Chem. Phys.* **1996**, *104*, 7296.

(38) Mujica, V.; Kemp, M.; Ratner, M. A. *J. Chem. Phys.* **1994**, *101*, 6849.

(39) Tian, W.; Datta, S.; Hong, S.; Reifenberger, R.; Henderson, J. I.; Kubiak, C. I. *J. Chem. Phys.* **1998**, *109*, 2874.

(40) Hall, L. E.; Reimers, J. R.; Hush, N. S.; Silverbrook, K. *J. Chem. Phys.* **2000**, *112*, 1510.

(41) Meir, Y.; Wingreen, N. S. *Phys. Rev. Lett.* **1992**, *68*, 2512.

(42) Troisi, A.; Ratner, M. A. *J. Chem. Phys.* **2006**, *125*, 214709.

(43) Reimers, J. R.; Hush, N. S. *J. Phys. Chem. B* **2001**, *105*, 8979.

(44) Bacon, A. D.; Zerner, M. C. *Theor. Chim. Acta* **1979**, *53*, 21.

(45) Ridley, J. E.; Zerner, M. C. *Theor. Chim. Acta* **1973**, *32*, 111.

(46) Solomon, G. C.; Reimers, J. R.; Hush, N. S. *J. Chem. Phys.* **2005**, *122*, 224502.

(47) Reimers, J. R.; Cai, Z.-L.; Bilic, A.; Hush, N. S. *Ann. N.Y. Acad. Sci.* **2003**, *1006*, 235.

(48) Bilic, A.; Reimers, J. R.; Hoft, R. C.; Ford, M. J. *J. Chem. Theory Comput.* **2006**, *2*, 1093.

(49) Cafe, P. F.; Reimers, J. R.; Bilic, A.; Crossley, M. J.; Blake, I.; Ulstrup, J.; Zhang, J.; Wackerbarth, H. *J. Phys. Chem. B* in preparation.

(50) Wang, Y.; Reimers, J. R.; Hush, N. S. *J. Phys. Chem. B* **2006**, submitted.

(51) Lambropoulos, N. A.; Reimers, J. R.; Hush, N. S. *J. Chem. Phys.* **2002**, *116*, 10277.

(52) Zhechkov, L.; Heine, T.; Patchkovskii, S.; Seifert, G.; Duarte, H. A. *J. Chem. Theory Comput.* **2005**, *1*, 841.

(53) Cui, Q.; Elstner, M.; Kaxiras, E.; Frauenheim, T.; Karplus, M. *J. Phys. Chem. B* **2001**, *105*, 569.

(54) Neumann, R.; Nobes, R. H.; Handy, N. C. *Mol. Phys.* **1996**, *87*, 1.

(55) Lee, A. M.; Handy, N. C. *J. Chem. Soc., Faraday Trans.* **1993**, *89*, 3999.

(56) Cai, Z.-L.; Reimers, J. R. *J. Chem. Phys.* **2000**, *112*, 527.

(57) Chermette, H.; Ciofini, I.; Mariotti, F.; Daul, C. *J. Chem. Phys.* **2001**, *114*, 1447.

(58) Ciofini, I.; Chermette, H.; Adamo, C. *Chem. Phys. Lett.* **2003**, *380*, 12.

(59) Gunnarsson, O.; Lundqvist, B. I. *Phys. Rev. B* **1976**, *13*, 4274.

(60) Perdew, J. P.; Wang, Y. *Phys. Rev. B* **1992**, *45*, 13244.

(61) Becke, A. D. *J. Chem. Phys.* **1993**, *98*, 5648.

(62) Whitehead, M. A. The Self-Interaction Correction Local Spin Density Approximation with VWN Correlation and Full Relativistic Corrections. In *Recent Advances in Density Functional Methods, Part 2*; Chong, D., Ed.; World Scientific: Singapore, 1997; p 229.

(63) Tozer, D. J.; Handy, N. C. *J. Chem. Phys.* **1998**, *109*, 10180.

(64) Tozer, D. J. *J. Chem. Phys.* **2000**, *112*, 3507.

(65) Casida, M. E.; Gutierrez, F.; Guan, J.; Gadea, F.-X.; Salahub, D.; Daudey, J.-P. *J. Chem. Phys.* **2000**, *113*, 7062.

(66) Yanai, T.; Tew, D. P.; Handy, N. C. *Chem. Phys. Lett.* **2004**, *393*, 51.

(67) Cai, Z.-L.; Tozer, D. J.; Reimers, J. R. *J. Chem. Phys.* **2000**, *113*, 7084.

(68) Bilic, A.; Reimers, J. R.; Hush, N. S. *J. Chem. Phys.* **2005**, *122*, 094708.

(69) Görling, A. *Phys. Rev. A* **1996**, *54*, 3912.

(70) Niehaus, T. A.; Suhai, S.; Della Sala, F.; Lugli, P.; Elstner, M.; Seifert, G.; Frauenheim, T. *Phys. Rev. B: Condens. Matter* **2001**, *63*, 085108/1.

(71) Niehaus, T. A.; Rohlfing, M.; Sala, F. D.; Di Carlo, A.; Frauenheim, T. *Phys. Rev. A* **2005**, 022508.

(72) Cai, Z.-L.; Sendt, K.; Reimers, J. R. *J. Chem. Phys.* **2002**, *117*, 5543.

(73) van Gisbergen, S. J. A.; Schipper, P. R. T.; Gritensko, O. V.; Baerends, E. J.; Snijders, J. D.; Champagne, B.; Kirtman, B. *Phys. Rev. Lett.* **1999**, *83*, 694.

(74) Dahlbom, M. G.; Reimers, J. R. *Mol. Phys.* **2005**, *103*, 1057.

(75) Cai, Z.-L.; Crossley, M. J.; Reimers, J. R.; Kobayashi, R.; Amos, R. D. *J. Phys. Chem. B* **2006**, *110*, 15624.

(76) Andreoni, W.; Curioni, A.; Gronbeck, H. *Int. J. Quantum Chem.* **2000**, *80*, 598.

(77) Grönbeck, H.; Curioni, A.; Andreoni, W. *J. Am. Chem. Soc.* **2000**, *122*, 3839.

(78) Fenter, P.; Schreiber, F.; Berman, L.; Scoles, G.; Eisenberger, P.; Bedzyk, M. J. *Surf. Sci.* **1998**, *412/413*, 213.

(79) Kluth, G. J.; Carraro, C.; Marboudian, R. *Phys. Rev. B* **1999**, *59*, R10449.

(80) Nishida, N.; Hara, M.; Sasabe, H.; Knoll, W. *Jpn. J. Appl. Phys.* **1996**, *35*, 5866.

(81) Fenter, P.; Eberhardt, A.; Eisenberger, P. *Science* **1994**, *266*, 1216.

(82) Yeganeh, M. S.; Dougal, S. M.; Polizzotti, R. S.; Rabinowitz, P. *Phys. Rev. Lett.* **1995**, *74*, 1811.

(83) Kuhnle, A.; Linderoth, T. R.; Hammer, B.; Besenbacher, F. *Nature* **2002**, *415*, 891.

(84) Akinaga, Y.; Nakajima, T.; Hirao, K. *J. Chem. Phys.* **2001**, *114*, 8555.

(85) Gottschalck, J.; Hammer, B. *J. Chem. Phys.* **2002**, *116*, 784.

(86) Hayashi, T.; Morikawa, Y.; Nozoye, H. *J. Chem. Phys.* **2001**, *114*, 7615.

(87) Noh, J.; Hara, M. *Langmuir* **2000**, *16*, 2045.

(88) Sellers, H.; Ulman, A.; Shnidman, Y.; Eilers, J. E. *J. Am. Chem. Soc.* **1993**, *115*, 9389.

(89) Yourdshahyan, Y.; Rappe, M. A. *J. Chem. Phys.* **2002**, *117*, 825.

(90) Yourdshahyan, Y.; Zhang, H. K.; Rappe, A. M. *Phys. Rev. B* **2001**, *63*, 081405.

(91) Kondoh, H.; Iwasaki, M.; Shimada, T.; Amemiya, K.; Yokoyama, T.; Ohta, T. *Phys. Rev. Lett.* **2003**, *90*, 066102.

(92) Roper, M. G.; Skegg, M. P.; Fisher, C. J.; Lee, J. J.; Dhanak, V. R.; Woodruff, D. P.; Jones, R. G. *Chem. Phys. Lett.* **2004**, *389*, 87.

(93) Maksymovych, P.; Sorescu, D. C.; Yates, J. T., Jr. *Phys. Rev. Lett.* **2006**, *97*, 146103.

(94) Molina, L. M.; Hammer, B. *Chem. Phys. Lett.* **2002**, *360*, 264.

(95) Reimers, J. R.; Hush, N. S. *Chem. Phys.* **1990**, *146*, 105.

(96) Zeng, J.; Hush, N. S.; Reimers, J. R. *J. Am. Chem. Soc.* **1996**, *118*, 2059.

(97) Zheng, G.; Frisch, M.; Morokuma, K. *Abstracts of Papers*, 232nd National Meeting of the American Chemical Society, San Francisco, CA, Sept 10−14, 2006; American Chemical Society: Washington, DC, 2006, COMP.

(98) Ryabov Vladimir, B. *Phys. Rev. E* **2002**, *66*, 016214.

(99) Sattin, F. *Comput. Phys. Commun.* **1997**, *107*, 253.